LEADER-FOLLOWER IMPEDANCE CONTROL FOR IMPROVING THE SOCIAL ACCEPTANCE OF MOBILE ROBOTS

Daniel Herrera*, Flavio Roberti†, Marcos Toibero‡, Ricardo Carelli§

*Instituto de Automática
Universidad Nacional de San Juan - CONICET
San Juan, Argentina

Emails: dherrera@inaut.unsj.edu.ar, froberti@inaut.unsj.edu.ar, mtoibero@inaut.unsj.edu.ar, rcarelli@inaut.unsj.edu.ar

Abstract— A complete characterization of the behavior in human-robot interactions (HRI) includes both: the behavior dynamics and the control laws that characterizes how the behavior is regulated with the perception data. In this way, this work proposes a leader-follower coordinate control based on an impedance control that allows to establish a dynamic relation between social forces and the motion error. For this, it is presented a scheme to identify the impedance based on fictitious social forces, which are described by distance-based potential fields. As part of the validation procedure, it is presented an experimental comparison to select the better of two different fictitious force structures. Finally, with the best fictitious force and its identified impedance, it is designed an impedance control for a mobile robot Pioneer 3AT®, which is programmed to follow a human in a structured scenario. According with the results, and, under the hypothesis that moving like humans will be acceptable by humans, it is believed that the proposed control improves the social acceptance of the robot for this kind of interaction.

Keywords— Human-robot interaction, Human dynamics, Social robotics, Impedance control.

1 Introduction

According to the proxemic studies developed by (Hall, 1963), the human respect social zones during different kind of interactions, i.e. social spaces depending of the task, the situation, and also of cultural or personal preferences.

In Robotics, this concept has been widely used. For example, (Chi-Pang et al., 2011) discusses different types of personal space for humans according to the situation. In (Ratsamee et al., 2013) it is proposed a human-fiendly navigation, where the concept of personal space or "hidden space" is used to prevent uncomfortable feelings when humans plan to avoid or interact with a robot. Even if it seems quite easy to respect this zones like solid barriers, it results inevitable the meddling in them when two individuals are interacting and moving. In this way, the comfort of the individual is not only guaranteed through the avoidance of this social zones, but also the involved dynamics during meddling events.

The dynamic relation that exists between an interaction force and the motion error is usually defined as impedance in robotics. The impedance allows to give specific dynamic qualities to the robotic motions. For example, in (Tsumugiwa et al., 2004) it is presented an impedance control of a robotic manipulator in a human-robot cooperative task system. Also, in teleoperation, it has been taken to improve the transparency by using an online variable impedance control as a natural sensor of human intention (Duchaine and Gosselin, 2007). The concept of impedance with fictitious forces has also been used to modify the desired velocity in robots, thus deviating the desired robot trajectory to avoid obstacles by considering a desired impedance characteristic (Tsuji et al., 1997). In this way, this paper proposes to describe the human-robot interaction through fictitious potential fields with impedance characteristics, where its flexible nature is determined by an impedance experimentally identified in human-human interactions.

In Section 2 the fictitious forces to be used as social repulsive zones are presented. These will be tested and compared to improve the identification of an impedance as defined in Section 3. Later, in Section 4 it is designed a dynamic control based on feedback linealization and impedance control. In the Section 5, the experimental results by programming a mobile robot Pioneer 3AT are presented. As part of this, an identification stage to define the fictitious force to be used, the desired impedance and the dynamical parameters of the robot is included. Finally in Section 6 the conclusions of the work are presented.

2 Fictitious forces

Based on the representations of fictitious forces given by the literature (Carelli et al., 2006), let's define two general fictitious force structures to describe the social repulsion between individuals. The first one corresponds to Gaussian functions piece-wise defined as

$$f_1^{(\mathrm{n})}(t) = \begin{cases} a\dfrac{\left(e^{-\frac{d^n(t)}{d_{\max}}} - e^{-d_{\max}^{n-1}}\right)}{1-e^{-d_{\max}^{n-1}}}, & \text{if} \quad d(t) < d_{\max} \\ 0, & \text{if} \quad d(t) \geq d_{\max} \end{cases} \quad (1)$$

and the second one to polynomial functions

$$f_2^{(n)}(t) = \begin{cases} a\left(1-\left(\dfrac{d(t)}{d_{\max}}\right)^n\right), & \text{if} \quad d(t) < d_{\max} \\ 0, & \text{if} \quad d(t) \geq d_{\max} \end{cases} \tag{2}$$

where $d(t)$ is the distance between humans, or well, between human and robot, in each time instant; $d_{\max}$ the maximal distance of action of the force; a is maximal value of the force, and, $n \in \mathcal{N}$ is the order of the functions. The previously defined functions are continuous and piece-wise defined to well establish the limits of action of the fictitious repulsive force. These general functions are used in the following Sections to define the best one to characterize an impedance effect.

3 Impedance with fictitious forces

The concept of impedance control aims at establishing the dynamic regulation between the motion and the interacting force of the robot with the environment. When a non-contact regulation is preferred fictitious forces are used instead, i.e., a virtual interaction. The linear impedance can be expressed as (Carelli et al., 2006), $f(t) = Z(p)\tilde{x}(t)$, where $p = d/dt$ is the time derivative operator, $f(t)$ is the interacting force of the robot with the environment, $\tilde{x}$ represents the robot motion error in relation to the specified trajectory, and, $Z(p) := Ip^2 + Bp + K$ is the impedance function, where I, B and K are the inertial, damping and spring constants respectively.

Concerning the human-human interaction context, it is considered that the impedance defines the interaction dynamics itself when a human is following another one, i.e., the linear impedance captures the inertial, damping and spring effects of this human relative motion. For this, it is identified the impedance as a parametric model as follows,

$$f(t) = \begin{bmatrix}\ddot{\tilde{x}}(t) & \dot{\tilde{x}}(t) & \tilde{x}(t)\end{bmatrix}\begin{bmatrix}I & B & K\end{bmatrix}^T, \tag{3}$$

then it results in a model with the form $\mathbf{Y} = \mathbf{T}\Theta$, which is identified in the following Sections by considering a recursive least squares algorithm (Wen-Chun and Neng-Yih, 2006).

To improve the identification it is considered only the data when $d(t) < d_{max}$, i.e. when the fictitious force has a non-zero value and a meddling event in the social space is occurring. In this way let's define a subspace $\mathcal{L} = \{t^* \mid d(t^*) < d_{max}\}$. In consequence the motion errors are defined as

$$\tilde{x} := d_d - d(t^*), \quad \dot{\tilde{x}} := \nu_{S/L}(t^*), \quad \ddot{\tilde{x}} := a_{S/L}(t^*),$$

where $d(t)$ are the measures of distance between leader and follower during the experiment, $d_d := \text{mean}(d(t))$ is considered as the desired following distance that is also used to define the action range of the fictitious forces, i.e. $d_{\max} := d_d$, and, $\nu_{S/L}(t^*), a_{S/L}(t^*)$ are the relative velocity and acceleration between leader and follower.

To take measures of these variables it is considered a one-dimension following during the human-human experiment. Concerning practical issues, this fact guarantees that the motion errors are correctly chosen, and in consequence the impedance is well defined.

4 Dynamic motion control for human following

4.1 Robot dynamic model

Consider that the dynamic model for a differential drive mobile robot is defined by (De la Cruz and Carelli, 2008)

$$\begin{bmatrix}\dot{x}_r \\ \dot{y}_r \\ \dot{\psi}_r \\ \dot{\nu}_r \\ \dot{\omega}_r\end{bmatrix} = \begin{bmatrix}\nu_r\cos\psi_r - a\omega_r\sin\psi_r \\ \nu_r\sin\psi_r - a\omega_r\cos\psi_r \\ \omega_r \\ \dfrac{\theta_3^{(r)}}{\theta_1^{(r)}}\omega_r^2 - \dfrac{\theta_4^{(r)}}{\theta_1^{(r)}}\nu_r \\ -\dfrac{\theta_5^{(r)}}{\theta_2^{(r)}}\nu_r\omega_r - \dfrac{\theta_6^{(r)}}{\theta_2^{(r)}}\omega_r\end{bmatrix} + \begin{bmatrix}0 & 0 \\ 0 & 0 \\ 0 & 0 \\ \dfrac{1}{\theta_1^{(r)}} & 0 \\ 0 & \dfrac{1}{\theta_2^{(r)}}\end{bmatrix}\begin{bmatrix}\nu_d \\ \omega_d\end{bmatrix} \tag{4}$$

where $\Theta_r = \{\theta_1^{(r)}, \theta_2^{(r)}, \theta_3^{(r)}, \theta_4^{(r)}, \theta_5^{(r)}, \theta_6^{(r)}\}$ are the parameters of the robot model, (x_r, y_r, ψ_r) its posture, $\{\nu_r, \omega_r\}$ its linear and angular velocity, and, $\{\nu_d, \omega_d\}$ its linear and angular velocity references.

4.2 Control of feedback linearization

If it is considered that the control objective is to keep a relative position to the human leader, then the output vector is defined by the robot position $\mathbf{x}_r = \begin{bmatrix}x_r & y_r\end{bmatrix}^T$.

Additionally by considering the robot model defined in (4), it can be expressed the first and second time derivative of the output as

$$\dot{\mathbf{x}}_r = \begin{bmatrix}\dot{x}_r \\ \dot{y}_r\end{bmatrix} = \mathbf{J}\mathbf{v}_r, \qquad \ddot{\mathbf{x}}_r = \mathbf{q} + \mathbf{J}\left(\mathbf{g} + \mathbf{H}\mathbf{u}_d\right) \tag{5}$$

with $\mathbf{v}_r = [\nu_r, \omega_r]^T$ the velocity vector of the robot, $\mathbf{u}_d = [\nu_d, \omega_d]^T$ its velocity references, and,

$$\mathbf{J} := \begin{bmatrix}\cos\psi_r & -a\sin\psi_r \\ \sin\psi_r & a\cos\psi_r\end{bmatrix},$$

$$\mathbf{q} := \begin{bmatrix}-u_r w_r\sin\psi_r - aw_r^2\cos\psi_r \\ u_r w_r\cos\psi_r - aw_r^2\sin\psi_r\end{bmatrix},$$

$$\mathbf{g} := \begin{bmatrix}\dfrac{\theta_3^{(r)}}{\theta_1^{(r)}}w_r^2 - \dfrac{\theta_4^{(r)}}{\theta_1^{(r)}}u_r \\ -\dfrac{\theta_5^{(r)}}{\theta_2^{(r)}}u_r w_r - \dfrac{\theta_6^{(r)}}{\theta_2^{(r)}}w_r\end{bmatrix}, \ \mathbf{H} := \begin{bmatrix}\dfrac{1}{\theta_1^{(r)}} & 0 \\ 0 & \dfrac{1}{\theta_2^{(r)}}\end{bmatrix}$$

If it is defined in (5) the following control of feedback linearization

$$\mathbf{u}_d := \mathbf{H}^{-1}\left[\mathbf{J}^{-1}\left(\mathbf{v} - \mathbf{q}\right) - \mathbf{g}\right]. \tag{6}$$

then the resultant system is an input-output linear system with the form $\ddot{\mathbf{x}}_r = \mathbf{v}$.
In this way, it remains to define the auxiliary input $\mathbf{v}$, which acts like an external loop as shown in Fig. 2. For this, it is proposed to use an impedance control, which allows to establish a dynamic relation between the fictitious force and the motion error during the following of the human leader, as detailed bellow.

4.3 Impedance control

Let's define the motion error in each coordinate axis $\tilde{\mathbf{x}} = [x_d - x_r, y_d - y_r]^T$ and the desired impedance

$$\mathbf{f}_{\text{desired}}(t) = \left(\mathbf{I}p^2 + \mathbf{B}p + \mathbf{K}\right)\tilde{\mathbf{x}}(t), \qquad (7)$$

where $\mathbf{I}$ is the inertia matrix, $\mathbf{B}$ the damping matrix, and, $\mathbf{K}$ the elasticity matrix, where $\mathbf{I} = \text{diag}(I, I)$, $\mathbf{B} = diag(B, B)$, $\mathbf{K} = diag(K, K)$ with $\{I, B, K\}$ identified as presented in Section 3. Additionally $x_d := x_L - d_d \cos\gamma$, $y_d := y_L - d_d \sin\gamma$, where, (x_L, y_L), (x_r, y_r) are the global position of the human leader and the robot follower respectively, and, γ is its relative orientation (see Fig. 1).

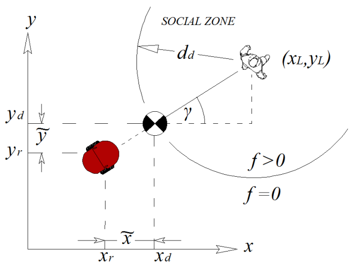

Figure 1: Leader-follower system.

To define the interaction social force, it is considered the center of the potential at (x_L, y_L), where the magnitude of the fictitious repulsive force is defined by (1) or (2) with direction γ. In this way, the force components in x, y are decomposed as follows $\mathbf{f}_{\text{social}}^{\{j\}} := [f_j^{(n)}(t)\cos\gamma, f_j^{(n)}(t)\sin\gamma]$, $j = \{1, 2\}$.

Once that the interaction force and the motion error are defined, it is proposed to define the auxiliary input $\mathbf{v}$ based on an impedance control as bellow

$$\mathbf{v} := \ddot{\mathbf{x}}_L + \mathbf{I}^{-1}\left(\mathbf{B}\dot{\tilde{\mathbf{x}}} + \mathbf{K}\tilde{\mathbf{x}} - \mathbf{f}_{\text{social}}^{\{j\}}\right) \qquad (8)$$

where $\dot{\tilde{\mathbf{x}}}$ is the time derivative of the motion error, and, $\ddot{\mathbf{x}}_L = [\ddot{x}_L, \ddot{y}_L]$ is the acceleration vector of the leader in the global framework. In this way, by substituting (8) in (6) is completely defined the dynamic motion control.

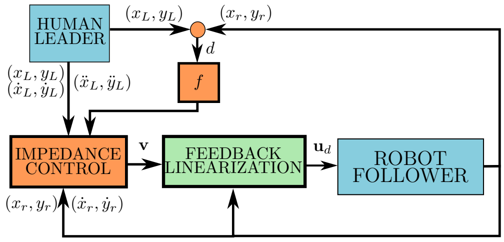

Figure 2: Scheme of control.

5 Experimental results

5.1 Experimental setup

For estimating the parameters of the impedance model (3), it is necessary to take measures of two humans, one following the other, and consequently to estimate the involved variables in the identification. For this, a range sensor LiDAR is located in the world space as shown in Fig. 3. This sensor is capable to take measures for a distance as long as 30 meters and in a scanning angle of 180° with a resolution of 0.5° or 1°.

Thus, the scenario consists in a structured environment that is horizontally scanned by a laser range sensor. So during the experiment, the scenario is only visited by the two involved participants, who are coming one after the other (see Fig. 3). The collected range points with high distance variations define the meddling of humans in the scenario. These points are classified by using an agglomerative hierarchical cluster tree, that later is used to classify in two groups according to its distance correlation.

Once the two groups are established, two characteristic points are defined through the mean point of each cluster. And finally, a $\alpha - \beta$ filter is used to get the positions, orientations and velocities of both participants (Kalata, 1984).

Figure 3: Experiment photo sequence.

5.2 Identification stage

5.2.1 Impedance identification

In Fig. 4 it is graphically presented the data obtained during the experiment. From this data, the motion error and the values of fictitious force are estimated.

Additionally these values are divided into two groups for the identification and validation procedures respectively as shown in Fig. 4. The data used in the identification procedure is presented

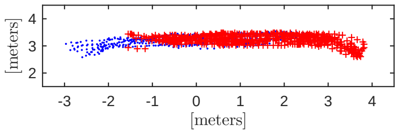

(a) Data for identification.

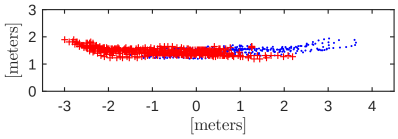

(b) Data for validation.

Figure 4: Overlapped experimental trajectories of the human leader (red sum "+" symbols) and follower (blue points) during the experiment.

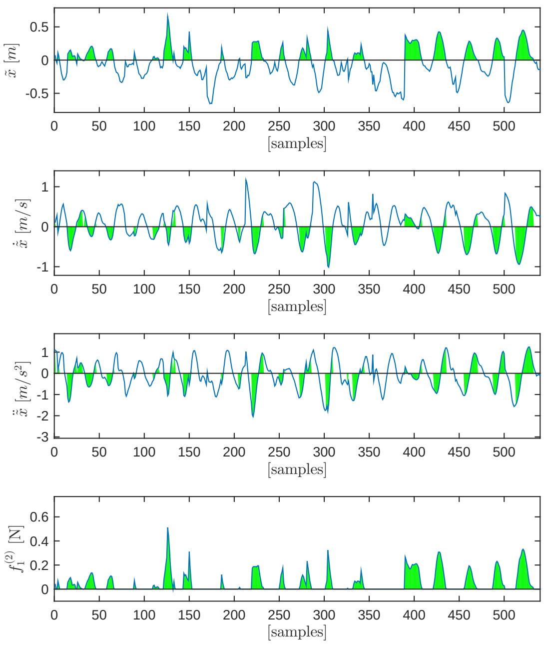

Figure 5: Experimental estimated variables.

in Fig. 5, and corresponds to 540 samples with a sample time of 0.1 seconds.

As mentioned, to improve the identification procedure it is only used the data during the periods when $d(t) < d_{\max}$, i.e., $f_j^{(n)} \neq 0$ (see marked zones in Fig. 5). This data is presented randomly until getting the parameters convergence as many times as it is necessary.

This identification procedure is repeated few times by considering different fictitious force models, and their results are compared by considering its variance (in *convergence* state) during the parameters identification procedure, and, by considering the impedance error given by the validation procedure.

Concerning the impedance error $\xi(t)$, it is defined and calculated as follows

$$\xi(t) = f_j^{(n)} - \left(I_j^{(n)} \ddot{\tilde{x}} + B_j^{(n)} \dot{\tilde{x}} + K_j^{(n)} \tilde{x} \right), \quad (9)$$

where $I_j^{(n)}, B_j^{(n)}, K_j^{(n)}$ are the parameters identified by considering the fictitious force $f_j^{(n)}, j = \{1, 2\}, n \in \mathcal{N}$ during the identification and validation procedure, and, $\{\ddot{\tilde{x}}, \dot{\tilde{x}}, \tilde{x}\}$ is experimental validation data. For each fictitious force it was considered a maximum value $a = 100[N]$ and a maximal range $d_{\max} = 1.55$ $[m]$. The obtained results are summarized in Table 1.

Table 1: Comparison between fictitious force models.

Fictitious force	Impedance Error		Parameter variance*		
	RMSE	r^{**}	σ_I	σ_B	σ_K
$f_1^{(2)}$	0.2564	0.9998	6.1458×10^{-5}	0.0025	0.0221
$f_1^{(4)}$	0.6664	0.9989	6.8462×10^{-4}	0.0286	0.1875
$f_1^{(10)}$	7.3994	0.9605	0.0236	0.4817	1.4054
$f_2^{(2)}$	1.1008	0.9987	8.3680×10^{-4}	0.0412	0.2081
$f_2^{(4)}$	4.9873	0.9890	0.0117	0.3077	1.0507
$f_2^{(10)}$	18.4340	0.9246	0.1270	2.3268	3.5112

*Variance of the parameters during RLS identification (last 400 samples).
**Mean correlation coefficients (r).

By analyzing the obtained values in Table 1 and by considering the aforementioned criteria, it is selected the fictitious force $f_1^{(2)}$ as the best one, and its results of identification and validation are presented in detail in Fig. 6 and Fig. 7 respectively. Finally, the obtained parameters results

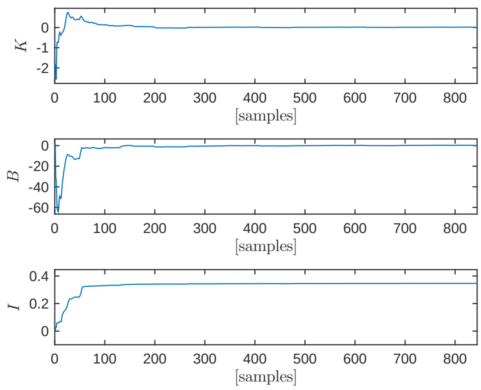

Figure 6: Recursive Least Squares Identification.

are selected to be: $K = 0.01, B = 0.19, I = 0.35$.

5.2.2 Identification of the robotic platform

To get experimental results with control of feedback linearization (6), it is necessary to identify the dynamic model of the robot. It is done by considering a filtered regression model as presented in (De la Cruz and Carelli, 2008). The data for the identification and validation procedures is obtained experimentally by using a differential drive model robot Pioneer 3AT, and, their parameters (used in the internal control loop) are: $\theta_1^{(r)} = 0.3037$, $\theta_2^{(r)} = 0.2768$, $\theta_3^{(r)} = -0.0004018$, $\theta_4^{(r)} = 0.9835$, $\theta_5^{(r)} = -0.003818$, $\theta_6^{(r)} = 1.0725$.

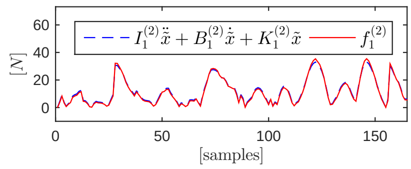

(a) Impedance (dashed blue line) and fictitious measured force (red line).

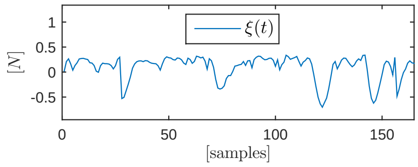

(b) Impedance error.

Figure 7: Experimental validation by considering $f_1^{(2)}$.

5.3 *Human-following control*

By considering the experimental scenario aforementioned, it is possible to determine the position of the human and derive the necessary variables to program the proposed control in a global framework (x, y). This information is sent to the mobile robotic platform Pioneer 3AT® which incorporates a low-level controller to regulate the linear and angular velocities. The interchange of data is made through a server-client connection, which allows to transfer the action commands to the robot and receive the odometer sensor data of the robot and the involved variables of the human motions of the scanned scenario (see Fig. 8).

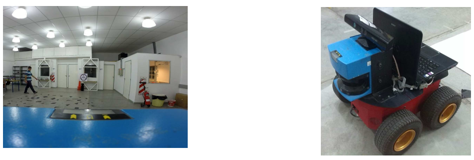

Figure 8: Experimental platform.

In this way, with the parameters identified in Sections 5.2.1 and 5.2.2, it is programmed a Pioneer 3AT with the previously design controller. The experiment consists in following a human while he is describing a quasi-circular trajectory during 715 samples with a sample time of 0.1 seconds.

Note that the escorting is not fixed to the behind position of the human, but it is adjusted dynamically by considering the relative orientation between human and robot (see Fig. 9 or watch a video clip in `https://youtu.be/7TdG-kzN3pE`). Even thought it is an interesting fact to choose the optimal human relative position from a "confort" sense, it has been not considered relevant to the present work, and it has been only focused on the dynamic aspects of the interaction.

Figure 9: Experimental photo sequence.

In Fig. 10 the motion errors are presented for each axis, where the events of meddling in the social zone are marked as repulsion forces, i.e, $f_x > 0$ and $f_y > 0$. Traditionally, a motion control is aimed to get a minimum motion error, however it is not a relevant fact when it is expected to generate specific dynamic behaviors. Consequently, this paper is only focused on validating the generated impedance during the robotic task. This way, in Fig. 11, the impedance generated by the robot and the measured fictitious force during the meddling events are compared, where the mean squared errors (RMSE) for each axis result to be $\text{RMSE}_x = 1.3429$ and $\text{RMSE}_y = 0.8966$, and the mean correlation coefficients are $r_x = 0.9882$ and $r_y = 0.9847$. Finally, the impedance errors are presented in Fig. 12, and, in Fig. 13 the control actions $\{\nu_d, \omega_d\}$ and the measured velocities of the mobile robot $\{\nu_r, \omega_r\}$ during the test.

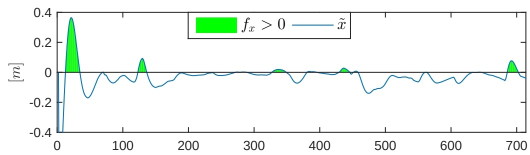

(a) x-axis.

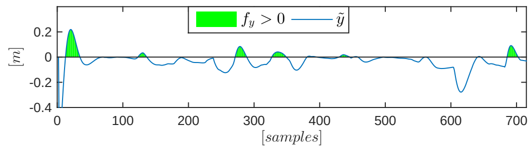

(b) y-axis.

Figure 10: Motion error.

6 Conclusions

In this paper it has been presented the design of a coordinate leader-follower control based on impedance control and feedback linearization that allows to establish a dynamic relation between the motion error and a fictitious social force. With the purpose to best characterize this behavior for the human-robot interaction, an experimental identification of the inertial, damping and elasticity properties of the impedance in human-human interactions has been proposed, where several models have been tested to select the appropriate for the impedance identification. Finally by using the identified parameters in the proposed control it has been programmed a mobile robot Pioneer 3AT

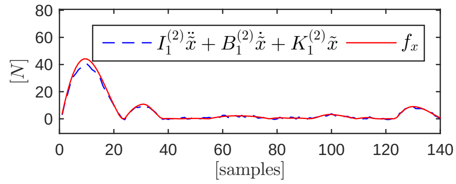

(a) x-axis.

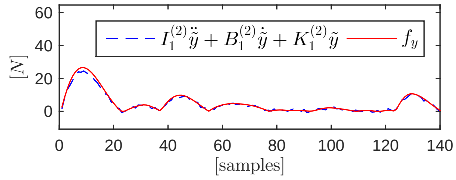

(b) y-axis.

Figure 11: Impedance (dashed blue line) and interaction force (red line).

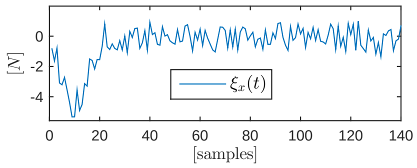

(a) x-axis.

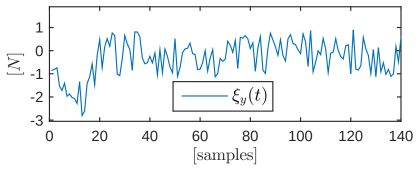

(b) y-axis.

Figure 12: Impedance errors.

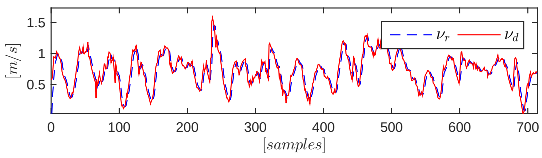

(a) Linear velocity.

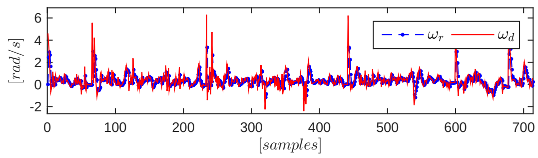

(b) Angular velocity.

Figure 13: Measured (blue dashed lines) and reference (red lines) robot velocities.

to follow a human in a structured scenario that is horizontally scanned by a LiDAR range sensor. The results show that the robot is capable to generate the identified interacting impedance, and consequently it is believed that the proposed control can improve the social acceptance by being able to imitate this human-human dynamic behavior.

References

Carelli, R., Santos-Victor, J., Roberti, F. and Tosetti, S. (2006). Direct visual tracking control of remote cellular robots, *Robotics and Autonomous Systems* **54**(10): 805–814.

Chi-Pang, L., Chen-Tun, C., Kuo-Hung, C. and Li-Chen, F. (2011). Human-centered robot navigation towards a harmoniously human robot coexisting environment, *IEEE Transactions on Robotics* **27**(1): 99–112.

De la Cruz, C. and Carelli, R. (2008). Dynamic model based formation control and obstacle avoidance of multi-robot systems, *Robotica* **26**(3): 345–356.

Duchaine, V. and Gosselin, C. M. (2007). General model of human-robot cooperation using a novel velocity based variable impedance control, *Second Joint EuroHaptics Conference and Symposium on Haptic Interfaces for Virtual Environment and Teleoperator Systems (WHC)*, pp. 446–451.

Hall, E. T. (1963). A system for the notation of proxemic behavior, *American Anthropologist* **65**(5): 1003–1026.

Kalata, P. R. (1984). The tracking index: A generalized parameter for $\alpha - \beta$ and $\alpha - \beta - \lambda$ target trackers, *IEEE Transactions on Aerospace and Electronic Systems* **AES-20**(2): 174–182.

Ratsamee, P., Mae, Y., Ohara, K., Kojima, M. and Arai, T. (2013). Social navigation model based on human intention analysis using face orientation, *IEEE/RSJ International Conference on Intelligent Robots and Systems (IROS)*, pp. 1682–1687.

Tsuji, T., Akamatsu, H. and Kaneko, M. (1997). Non-contact impedance control for redundant manipulators using visual information, *IEEE International Conference on Robotics and Automation*, Vol. 3, pp. 2571–2576.

Tsumugiwa, T., Yokogawa, R. and Yoshida, K. (2004). Stability analysis for impedance control of robot for human-robot cooperative task system, *IEEE/RSJ International Conference on Intelligent Robots and Systems (IROS 2004)*, Vol. 4, pp. 3883–3888.

Wen-Chun, Y. and Neng-Yih, S. (2006). Bi-loop recursive least squares algorithm with forgetting factors, *IEEE Signal Processing Letters* **13**(8): 505–508.